Title
SOURCE PROVENANCE OF OBSIDIAN ARTIFACTS FROM ARCHAEOLOGICAL SITES IN WASHINGTON COUNTY, SOUTHWESTERNUTAH

Author
Shackley, M. Steven

Publication Date
2020-05-05

GEOARCHAEOLOGICAL XRF LAB
A GREEN SOLAR FACILITY

GEOARCHAEOLOGICAL X-RAY FLUORESCENCE SPECTROMETRY LABORATORY
8100 Wyoming Blvd., Ste M4-158 Albuquerque, NM 87113
USA

SOURCE PROVENANCE OF OBSIDIAN ARTIFACTS FROM ARCHAEOLOGICAL SITES IN WASHINGTON COUNTY, SOUTHWESTERN UTAH

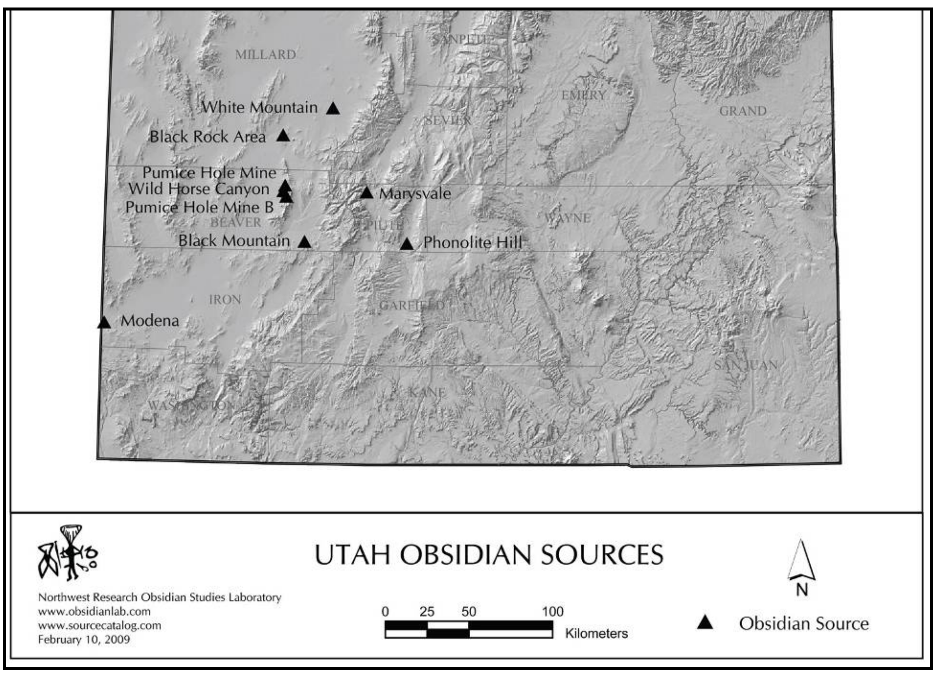

by

M. Steven Shackley, Ph.D., Director
Geoarchaeological XRF Laboratory
Albuquerque, New Mexico

Report Prepared for

Amber Van Alfen
Color Country District Office
Bureau of Land Management
St. George, Utah

5 May 2020

INTRODUCTION

The analysis here of 65 artifacts, 64 obsidian, from archaeological contexts in Washington County, southwest Utah indicates procurement of the raw material for production of the artifacts from southeastern Nevada, and southwestern Utah, essentially some of the nearest regional sources of archaeological obsidian (Tables 1 and 2, Figures 1 and 2). All of the five sources detected in this assemblage, are major source localities, many that produced obsidian nodules over 10 cm in minimum diameter (see Johnson and Wagner 2005). One artifact was not produced from obsidian, and one was too small to allow for confident source assignment (Davis et al. 2011; see Table 1 here). Note that there are two sources with similar names: Black Mountain in Millard County, Utah, and Black Rock Desert in Beaver County, Utah (see Figure 2). The results here are very different from those reported from sites in Grand and San Juan Counties, Utah on the eastern side of the state likely due to cultural and social network patterns (Shackley 2016).

LABORATORY SAMPLING, ANALYSIS AND INSTRUMENTATION

All archaeological samples are analyzed whole. The results presented here are quantitative in that they are derived from "filtered" intensity values ratioed to the appropriate x-ray continuum regions through a least squares fitting formula rather than plotting the proportions of the net intensities in a ternary system (McCarthy and Schamber 1981; Schamber 1977). Or more essentially, these data through the analysis of international rock standards, allow for inter-instrument comparison with a predictable degree of certainty (Hampel 1984; Shackley 2011).

All analyses for this study were conducted on a ThermoScientific *Quant'X* EDXRF spectrometer, located at the Geoarchaeological XRF Laboratory, Albuquerque, New Mexico. It is equipped with a thermoelectrically Peltier cooled solid-state Si(Li) X-ray detector, with a 50 kV, 50 W, ultra-high-flux end window bremsstrahlung Rh target X-ray tube and a 76 µm (3 mil) beryllium (Be) window (air cooled), that runs on a power supply operating 4-50 kV/0.02-1.0 mA at 0.02 increments. The spectrometer is equipped with a 200 l min^{-1} Edwards vacuum pump, allowing for the analysis of lower-atomic-weight elements between sodium (Na) and scandium (Sc). Data acquisition is accomplished with a pulse processor and an analogue-to-digital converter. Elemental composition is identified with digital filter background removal, least squares empirical peak deconvolution, gross peak intensities and net peak intensities above background.

For the analysis of mid Zb condition elements Ti-Nb, Pb, Th, the x-ray tube is operated at 30 kV, using a 0.05 mm (medium) Pd primary beam filter in an air path at 100 seconds livetime generally using an 8.8 mm tube collimator to generate x-ray intensity $K\alpha_1$-line data for elements titanium (Ti), manganese (Mn), iron (as $Fe_2O_3^T$), cobalt (Co), nickel (Ni), copper, (Cu), zinc, (Zn), gallium (Ga), rubidium (Rb), strontium (Sr), yttrium (Y), zirconium (Zr), niobium (Nb), lead (Pb), and thorium (Th). Not all these elements are reported since their values in many volcanic rocks are very low. Trace element intensities were converted to concentration estimates by employing a quadratic calibration line ratioed to the Compton scatter established for each element from the analysis of international rock standards certified by the National Institute of Standards and Technology (NIST), the US. Geological Survey (USGS), Canadian Centre for Mineral and Energy Technology, and the Centre de Recherches Pétrographiques et Géochimiques in France (Govindaraju 1994). Line fitting is quadratic (XML) for all elements. When barium (Ba) and cerium (Ce) is analyzed in the High Zb condition, the Rh tube is operated at 50 kV and up to 1.0 mA, ratioed to the bremsstrahlung region (see Davis 2011; Shackley 2011). Further details concerning the petrological choice of these elements in North American obsidians is available in Shackley (1988, 1995, 2005; also Mahood and Stimac 1991; and Hughes and Smith 1993, and http://swxrflab.net/swobsrcs.htm). Nineteen specific pressed powder standards are used for the best fit regression calibration for elements Ti-Nb, Pb, Th, Ba, and Ce include G-2 (basalt), AGV-2 (andesite), GSP-2 (granodiorite), SY-2 (syenite), BHVO-2 (hawaiite), STM-1 (syenite), QLO-1 (quartz latite), RGM-1 (obsidian), W-2 (diabase), BIR-1 (basalt), SDC-1 (mica schist), TLM-1 (tonalite), SCO-1 (shale), NOD-A-1 and NOD-P-1 (manganese) all US Geological Survey standards, NIST-278 (obsidian), U.S. National Institute of Standards and Technology, BE-N (basalt) from the Centre de Recherches Pétrographiques et Géochimiques in France, and JR-1 and JR-2 (obsidian) from the Geological Survey of Japan (Govindaraju 1994).

The data from the WinTrace™ software were translated directly into Excel for Windows software for manipulation and on into SPSS for Windows (Release 21) and JMP 12.0.1 for statistical analyses. In order to evaluate these quantitative determinations, machine data were compared to measurements of known standards during each run. RGM-1 a USGS rhyolite standard is analyzed during each sample run of ≤ 19 for obsidian artifacts to check machine calibration (Table 1).

Source assignments were made by reference to the laboratory data base (see Shackley 1995, 2005, online at http://swxrflab.net/swobsrcs.htm; Skinner and Thatcher 2005; and the Skinner/Shackley North American obsidian source database; see Table 1 and Figure 1). Further information on the laboratory instrumentation can be found at: http://swxrflab.net/anlysis.htm. Trace element data exhibited in Table 1 are reported in parts per million (ppm), a quantitative measure by weight.

REFERENCES CITED

Davis, M.K., T.L. Jackson, M.S. Shackley, T. Teague, and J. Hampel

2011 Factors Affecting the Energy-Dispersive X-Ray Fluorescence (EDXRF) Analysis of Archaeological Obsidian. In *X-Ray Fluorescence Spectrometry (XRF) in Geoarchaeology*, edited by M.S. Shackley, pp. 45-64. Springer, New York.

Govindaraju, K.

1994 1994 Compilation of Working Values and Sample Description for 383 Geostandards. *Geostandards Newsletter* 18 (special issue).

Hampel, Joachim H.

1984 Technical Considerations in X-ray Fluorescence Analysis of Obsidian. In *Obsidian Studies in the Great Basin*, edited by R.E. Hughes, pp. 21-25. Contributions of the University of California Archaeological Research Facility 45. Berkeley.

Hildreth, W.

1981 Gradients in Silicic Magma Chambers: Implications for Lithospheric Magmatism. *Journal of Geophysical Research* 86:10153-10192.

Hughes, R.E., and R. L. Smith

1993 Archaeology, Geology, and Geochemistry in Obsidian Provenance Studies. *In Scale on Archaeological and Geoscientific Perspectives*, edited by J.K. Stein and A.R. Linse, pp. 79-91. Geological Society of America Special Paper 283.

Johnson, L., and D.L. Wagner

2005 Obsidian Source Characterization Study. In *Fingerprints in the Great Basin: The Nellis Air Force Base Regional Obsidian Source Study*, edited by L. Haarklau, L. Johnson, and D.L. Wagner, pp. 25-50. U.S. Army Corps of Engineers, Fort Worth District, Fort Worth, Texas.

Mahood, Gail A., and James A. Stimac

1990 Trace-Element Partitioning in Pantellerites and Trachytes. *Geochemica et Cosmochimica Acta* 54:2257-2276.

McCarthy, J.J., and F.H. Schamber

1981 Least-Squares Fit with Digital Filter: A Status Report. In *Energy Dispersive X-ray Spectrometry*, edited by K.F.J. Heinrich, D.E. Newbury, R.L. Myklebust, and C.E. Fiori, pp. 273-296. National Bureau of Standards Special Publication 604, Washington, D.C.

Schamber, F.H.

1977 A Modification of the Linear Least-Squares Fitting Method which Provides Continuum Suppression. In *X-ray Fluorescence Analysis of Environmental Samples*, edited by T.G. Dzubay, pp. 241-257. Ann Arbor Science Publishers.

Shackley, M. Steven

1988 Sources of Archaeological Obsidian in the Southwest: An Archaeological, Petrological, and Geochemical Study. *American Antiquity* 53:752-772.

1995 Sources of Archaeological Obsidian in the Greater American Southwest: An Update and Quantitative Analysis. *American Antiquity* 60(3):531-551.

2005 *Obsidian: Geology and Archaeology in the North American Southwest*. University of Arizona Press, Tucson.

2011 An Introduction to X-Ray Fluorescence (XRF) Analysis in Archaeology. In *X-Ray Fluorescence Spectrometry (XRF) in Geoarchaeology*, edited by M.S. Shackley, pp. 7-44. Springer, New York.

2016 Source Provenance of Obsidian Artifacts from Archaeological Sites in Grand and San Juan Counties, Utah. Report prepared for the BLM Canyon Country Office, Moab, Utah.

Skinner, C.E., and J.J. Thatcher
2005 X-ray Fluorescence Trace Element Provenance Analysis of Geological Sources of Obsidian. In *Fingerprints in the Great Basin: The Nellis Air Force Base Regional Obsidian Source Study*, edited by L. Haarklau, L. Johnson, and D.L. Wanger, Appendix A-1. U.S. Army Corps of Engineers, Fort Worth District, Fort Worth, Texas.

Table 1. Elemental concentrations for all archaeological samples by site and sample number, and USGS RGM-1 rhyolite standard.

Sample	Site	Ti	Mn	Fe	Rb	Sr	Y	Zr	Nb	Ba	Pb	Th	Source
2	42WS4095	1322	445	11945	219	51	22	116	20	113	35	26	Wild Horse Canyon, UT
4	42WS4095	989	352	11769	210	86	36	122	19	568	32	25	Modena (Panaca Summit), UT
5	42WS4095	1051	342	11997	221	91	29	123	19	552	30	40	Modena (Panaca Summit), UT
6	42WS4095	1208	341	11784	208	89	28	118	18	486	27	42	Modena (Panaca Summit), UT
7	42WS4095	993	303	11195	190	80	32	119	19	569	26	40	Modena (Panaca Summit), UT
9	42WS4095	1124	363	12077	232	94	32	126	20	528	39	29	Modena (Panaca Summit), UT
10	42WS4095	1113	415	11423	206	45	16	122	26	111	31	32	Wild Horse Canyon, UT
11	42WS4095	964	390	11193	206	49	27	116	25	144	33	27	Wild Horse Canyon, UT
12	42WS4095	942	327	11461	192	78	34	117	20	574	27	30	Modena (Panaca Summit), UT
13	42WS4095	1057	378	11471	209	50	21	119	24	114	29	26	Wild Horse Canyon, UT
14	42WS4095	1009	298	11453	199	86	33	126	18	592	26	34	Modena (Panaca Summit), UT
15	42WS4095	975	340	11714	223	89	27	131	20	557	28	16	Modena (Panaca Summit), UT
16	42WS4095	1085	335	11760	218	90	33	122	22	548	31	31	Modena (Panaca Summit), UT
17	42WS4095	982	409	11605	220	54	21	119	21	233	34	22	Wild Horse Canyon, UT
18	42WS4095	1097	378	12122	238	93	34	135	20	583	32	42	Modena (Panaca Summit), UT
19	42WS4095	968	321	11846	219	91	27	125	14	589	28	29	Modena (Panaca Summit), UT
20	42WS4095	786	331	11248	189	82	29	116	18	572	26	26	Modena (Panaca Summit), UT
22	42WS4095	994	333	11862	223	86	24	131	23	545	30	33	Modena (Panaca Summit), UT
21	42WS4095	810	285	10861	178	82	27	110	18	596	25	33	Modena (Panaca Summit), UT
23	42WS4095	1192	332	10033	212	90	34	126	15	536	31	30	Modena (Panaca Summit), UT
24	42WS4095	1224	335	10222	220	93	36	125	19	555	28	29	Modena (Panaca Summit), UT

Sample	Site	Ti	Mn	Fe	Rb	Sr	Y	Zr	Nb	Ba	Pb	Th	Source
25	42WS4095	1109	316	9507	195	80	30	124	21	541	24	30	Modena (Panaca Summit), UT
26	42WS4095	1053	321	9329	196	85	31	127	20	593	24	27	Modena (Panaca Summit), UT
27	42WS4095	1206	374	10900	236	93	32	127	19	564	32	30	Modena (Panaca Summit), UT
29	42WS4095	1219	322	9697	188	80	32	121	20	572	25	36	Modena (Panaca Summit), UT
30	42WS4095	1195	321	9901	213	88	29	116	18	568	25	26	Modena (Panaca Summit), UT
31	42WS4095	1252	322	10178	210	84	31	133	18	538	33	38	Modena (Panaca Summit), UT
32A	42WS4095	1423	356	10766	206	83	29	105	15	470	29	33	Modena (Panaca Summit), UT
32B	42WS4095	1625	407	11895	224	84	25	119	17	417	37	34	Modena (Panaca Summit), UT
33	42WS4095	1480	347	9949	190	80	32	109	19	405	33	29	Modena (Panaca Summit), UT
34	42WS4095	1196	317	10155	212	87	30	130	26	600	29	24	Modena (Panaca Summit), UT
35	42WS4095	1259	330	10965	210	86	29	132	17	372	30	39	Modena (Panaca Summit), UT
36A	42WS4095	1172	338	10099	205	87	28	115	17	616	26	38	Modena (Panaca Summit), UT
36B	42WS4095	1470	365	10894	217	89	29	125	20	527	31	40	Modena (Panaca Summit), UT
36C	42WS4095	1297	466	10791	283	12	55	92	29	0	43	35	Black Rock Desert, UT
37	42WS4095	1050	516	11285	301	21	52	98	27	0	47	36	Black Rock Desert, UT
1	42WS4096	1103	363	8864	197	43	19	120	24	186	30	28	Wild Horse Canyon, UT
2	42WS4096	1340	335	10005	151	64	28	171	31	593	21	26	Wild Horse Canyon, UT
3	42WS4096	1229	337	10175	207	86	29	122	15	570	30	31	Modena (Panaca Summit), UT
4	42WS4096	1111	298	9662	206	86	28	126	16	603	23	37	Modena (Panaca Summit), UT
5	42WS4096	1385	365	9875	211	49	27	119	23	240	33	29	Wild Horse Canyon, UT
6	42WS4096	1186	348	10426	210	85	30	128	16	538	33	34	Modena (Panaca Summit), UT
7	42WS4096	949	430	9984	282	19	56	104	32	0	38	26	Black Rock Desert, UT

Sample	Site	Ti	Mn	Fe	Rb	Sr	Y	Zr	Nb	Ba	Pb	Th	Source
8	42WS4096	1265	326	10308	211	87	26	125	23	584	28	35	Modena (Panaca Summit), UT
9	42WS4096	1210	321	10476	218	91	31	128	22	533	35	31	Modena (Panaca Summit), UT
10	42WS4096	1235	316	12551	197	25	53	204	30	159	19	36	Kane Spring Wash, Var 1, NV[1]
11	42WS4096	1314	409	10078	208	52	24	121	22	212	31	29	Wild Horse Canyon, UT
12	42WS4096	1402	390	9766	213	45	19	109	18	131	31	19	Wild Horse Canyon, UT
13	42WS4096	1245	309	12402	218	51	33	161	34	275	25	32	Wild Horse Canyon, UT
14	42WS4096	1067	314	9607	200	86	31	129	19	637	26	26	Modena (Panaca Summit), UT
15	42WS4096	1161	404	9662	211	49	23	122	21	220	32	31	Wild Horse Canyon, UT
16	42WS4096	1769	236	10983	156	20	40	131	30	152	22	20	too small
1	42WS4097	657	146	5227	0	13	7	26	1	76	14	4	not obsidian
2	42WS4097	1181	329	9855	205	86	28	128	24	616	28	36	Modena (Panaca Summit), UT
3	42WS4097	1058	339	8747	187	43	26	116	20	224	26	21	Wild Horse Canyon, UT
4	42WS4097	1077	317	9491	202	88	31	123	25	630	28	37	Modena (Panaca Summit), UT
5	42WS4097	1109	300	9535	207	88	32	131	26	590	27	33	Modena (Panaca Summit), UT
6	42WS4097	898	397	9267	254	18	54	100	34	19	28	38	Black Rock Desert, UT
7	42WS4097	845	395	9662	272	19	55	99	33	33	34	31	Black Rock Desert, UT
8	42WS4097	1132	296	9709	192	81	32	124	25	599	24	33	Modena (Panaca Summit), UT
11	42WS4097	1111	304	9462	199	86	29	128	26	589	25	35	Modena (Panaca Summit), UT
12	42WS4097	1125	314	9811	206	87	26	132	18	616	26	34	Modena (Panaca Summit), UT
14A	42WS4097	788	430	9840	305	15	64	111	39	15	42	42	Black Rock Desert, UT
14B	42WS4097	1028	336	9504	205	83	26	124	20	615	25	25	Modena (Panaca Summit), UT
17	42WS4097	1100	369	9260	201	44	24	121	20	224	30	19	Wild Horse Canyon, UT

Sample	Site	Ti	Mn	Fe	Rb	Sr	Y	Zr	Nb	Ba	Pb	Th	Source
RGM1-S4		1589	292	13377	147	109	22	224	6	791	23	12	standard
RGM1-S4		1567	284	13143	142	106	25	219	7	760	20	8	standard

[1] Kane Spring Wash caldera obsidian sources exhibit two distinctive elemental compositions. The type in this assemblage is called "Variety 1" by Johnson and Wagner (2005). See also Figure 2.

Table 2. Crosstabulation of site by source. Does not include the one non-obsidian sample and the one too small for source assignment.

Source		Site 42WS4095	42WS4096	42WS4097	Total
Modena (Panaca Summit), UT	Count	29	6	7	42
	% within Source	69.0%	14.3%	16.7%	100.0%
	% within Site	80.6%	40.0%	58.3%	66.7%
	% of Total	46.0%	9.5%	11.1%	66.7%
Wild Horse Canyon, UT	Count	5	6	2	13
	% within Source	38.5%	46.2%	15.4%	100.0%
	% within Site	13.9%	40.0%	16.7%	20.6%
	% of Total	7.9%	9.5%	3.2%	20.6%
Black Rock Desert, UT	Count	2	1	3	6
	% within Source	33.3%	16.7%	50.0%	100.0%
	% within Site	5.6%	6.7%	25.0%	9.5%
	% of Total	3.2%	1.6%	4.8%	9.5%
Black Mountain, UT	Count	0	1	0	1
	% within Source	0.0%	100.0%	0.0%	100.0%
	% within Site	0.0%	6.7%	0.0%	1.6%
	% of Total	0.0%	1.6%	0.0%	1.6%
Kane Spring Wash, Var 1, NV	Count	0	1	0	1
	% within Source	0.0%	100.0%	0.0%	100.0%
	% within Site	0.0%	6.7%	0.0%	1.6%
	% of Total	0.0%	1.6%	0.0%	1.6%
Total	Count	36	15	12	63
	% within Source	57.1%	23.8%	19.0%	100.0%
	% within Site	100.0%	100.0%	100.0%	100.0%
	% of Total	57.1%	23.8%	19.0%	100.0%

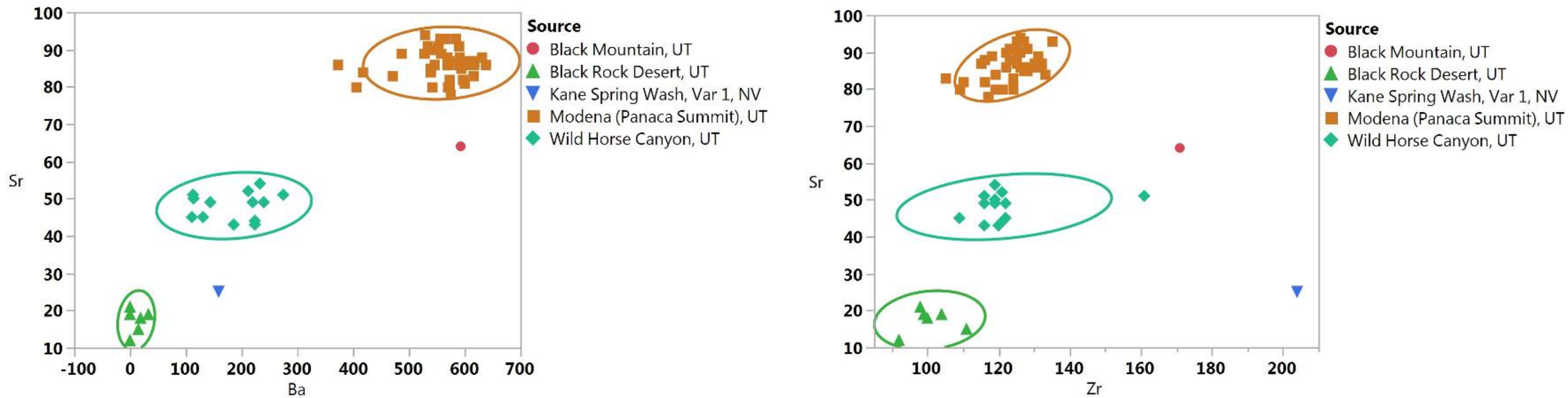

Figure 1. Ba/Sr and Zr/Sr bivariate plots of the archaeological samples and source assignments. Confidence ellipses at 95%.

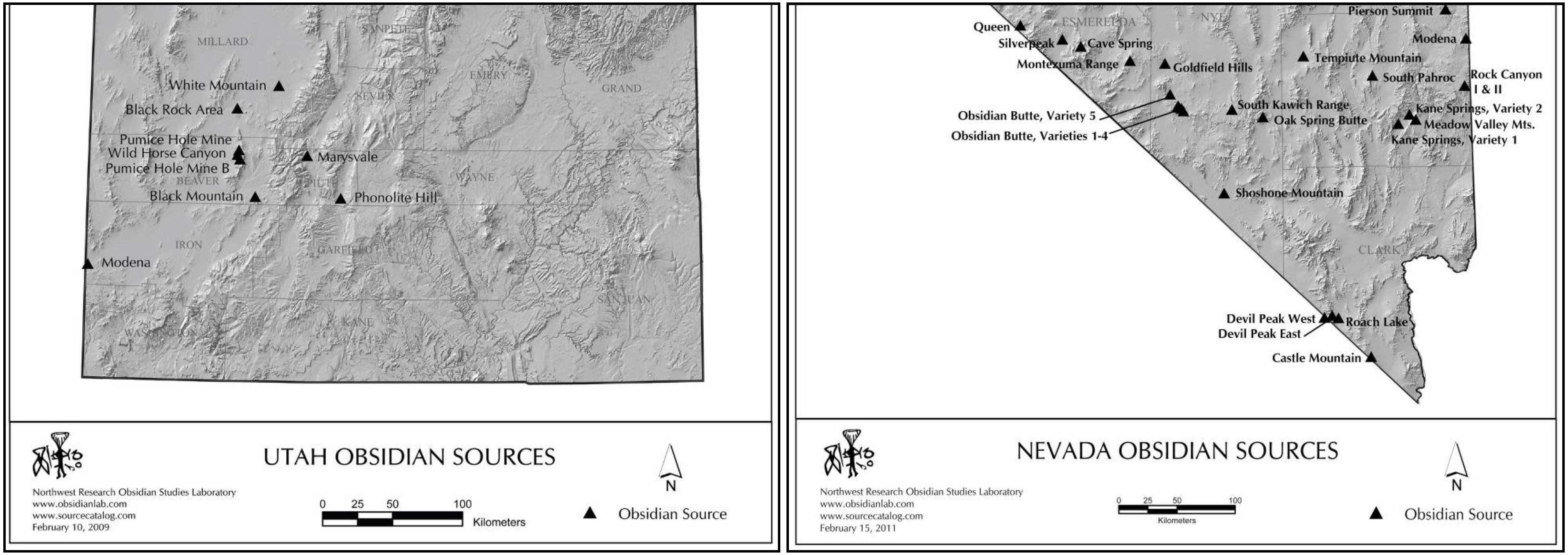

Figure 2. Location of sources of archaeological obsidian including those in this assemblage in southern Utah (left) and southern Nevada (right). From the Northwest Obsidian Studies Laboratory web (https://www.sourcecatalog.com/image_maps/index.html).